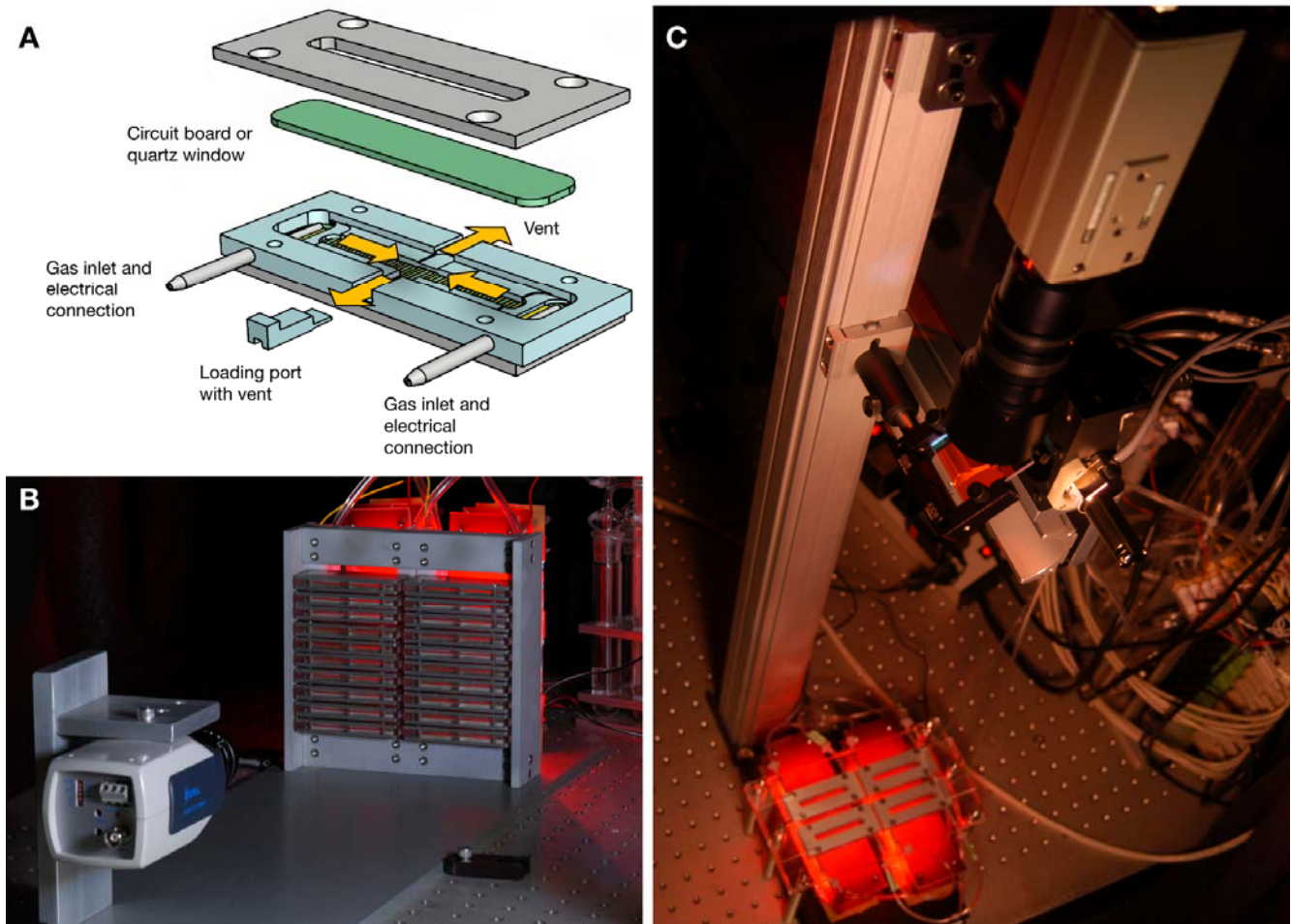


## Supplemental Data

### Writing Memories with Light-Addressable

### Reinforcement Circuitry

Adam Claridge-Chang, Robert D. Roorda, Eleftheria Vrontou, Lucas Sjulson, Haiyan Li, Jay Hirsh, and Gero Miesenböck



**Figure S1. Experimental Apparatus**

(A) Exploded view of a behavioral chamber. Flies are loaded through a lateral port and viewed side-on through transparent polycarbonate walls. Air/odor mixtures enter the chamber through inlets at the ends and exit through vents at the center, defining a 5-mm choice zone. Electric shock is delivered via floor and ceiling circuit boards. In photostimulation experiments, the circuit boards are replaced with quartz panes.

(B) In electric shock conditioning experiments, 20 flies are tested simultaneously in 20 chambers. The chambers are arranged into two side-by-side stacks by slotting their metal air/odor inlet tubes into gas distribution manifolds; the gas tubes also serve as electrical leads. The array is backlit by infrared LEDs (red LEDs shown for display purposes only) and viewed side-on by a CCD camera. Fly coordinates are calculated from video images.

(C) In optical conditioning experiments, four flies are tested simultaneously in four chambers. The chambers are arranged flat on a clear acrylic platform and back-illuminated by infrared LEDs (red LEDs shown for display purposes only). The chambers are viewed from above by a CCD camera; position data are calculated from video images. Optical stimuli are delivered by an ultraviolet laser. Upon entry of a fly into the reinforced odor stream, the fly's coordinates are automatically fed to a pair of galvanometric scan mirrors to position the beam, and the laser is activated for 10 ms.

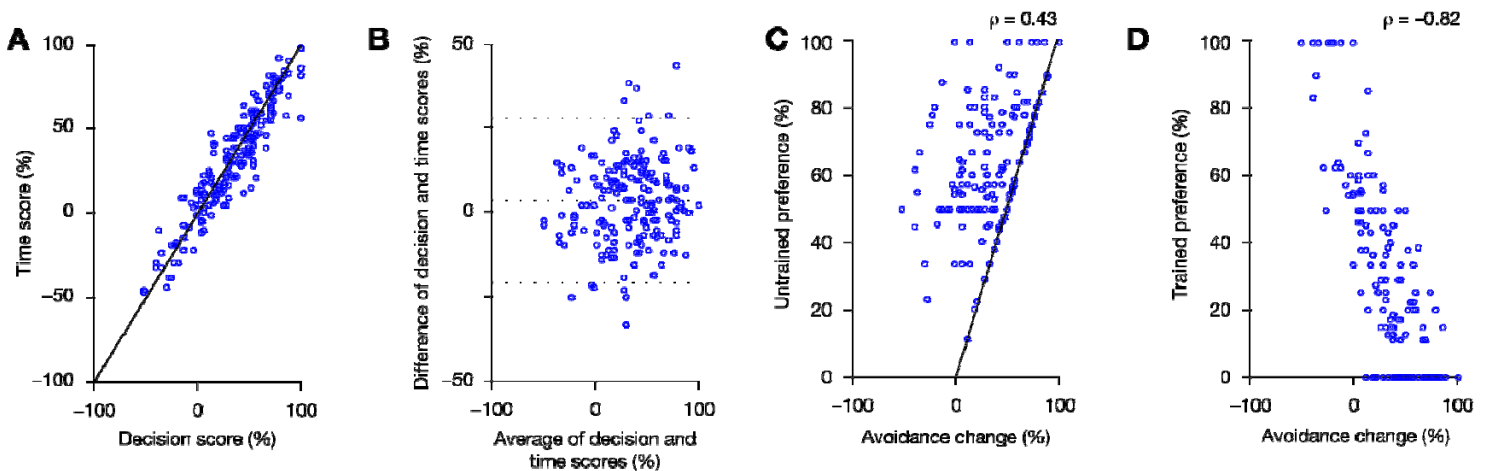


### Figure S2. Quantifying Changes in Odor Avoidance to Measure Learning

Two hundred flies were trained in an action-contingent regime to avoid MCH; 190 flies met the inclusion criteria for analysis (see Experimental Procedures). Two measures of training-induced avoidance changes were calculated: a time score, which quantifies the percentage of time spent in odor A during a test interval:  $(\text{time}_{\text{odorA}} / \text{time}_{\text{interval}}) \times 100 \%$ ; and a decision score, which is based on the percentage of decisions in favor of odor A during a test interval. A decision was

counted every time a fly entered and exited the central choice zone. Entry into odor A from the choice zone, either as the result of a reversal or a traversal, was tallied in favor of that odor's choice percentage:  $(\text{decisions}_{\text{odorA}} / \text{decisions}_{\text{interval}}) \times 100 \%$ . Time and decision scores are learning indices, obtained by subtracting the post-training preference from the pre-training preference, giving a percentage change. The results of aversive conditioning are reported as negative preference – that is, positive avoidance – changes.

(A) Scatterplot of time and decision scores. The two measures cluster tightly around the equality line.

(B) Scatterplot of the difference between decision and time scores against their mean. The near-equality of decision and time scores (A), together with the lack of an obvious relation between their difference and mean, suggests that these measures may be used interchangeably [Bland, J.M., and Altman, D.G. (1986). Statistical methods for assessing agreement between two methods of clinical measurement. *Lancet Feb. 8 (1)*, 307-310]. Dotted lines mark the mean difference (3.7 %) and 95 % limits of agreement (–21.0 % and 28.4 %). Because the decision measure inherently requires at least one choice to be made in a 2-min trial period, providing a simple filter against immobile flies, decision-based avoidance changes were generally reported.

(C, D) Relationships between untrained (C) and trained preference (D) and avoidance change. The diagonal in C represents the maximal avoidance change attainable for a fly with a given untrained preference: a fly can only reduce its conditioned preference to 0 % (that is, display perfect odor avoidance). Its untrained preference thus places a ceiling on the maximum possible avoidance change. Despite this, avoidance change is correlated more tightly with the animal's conditioned (D) than its untrained preference (C), suggesting that such ceiling effects are minor ( $\rho$  = Spearman's rank correlation coefficient).

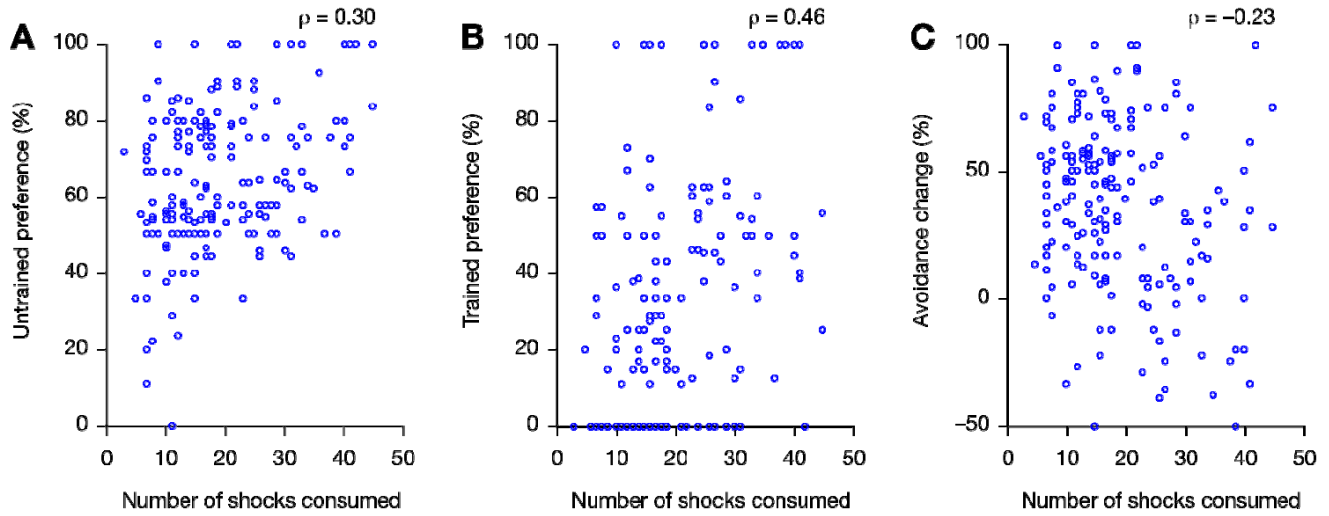


### Figure S3. Relationships between Shock Consumption, Odor Preference, and Learning

Two hundred flies were trained in an action-contingent regime to avoid MCH; 190 flies met the inclusion criteria for analysis (see Experimental Procedures).

(A, B) Animals with more pronounced untrained and trained preferences for MCH tend to consume more shocks; this may simply reflect the greater proclivities of these individuals for entering MCH.

(C) Flies exhibiting large avoidance changes tend to consume fewer shocks than flies whose MCH preference remains high despite reinforcement, suggesting that “fast learners” can be taught quickly to avoid the shock-associated odor (see also Figure 3B). ( $\rho$  = Spearman’s rank correlation coefficient).

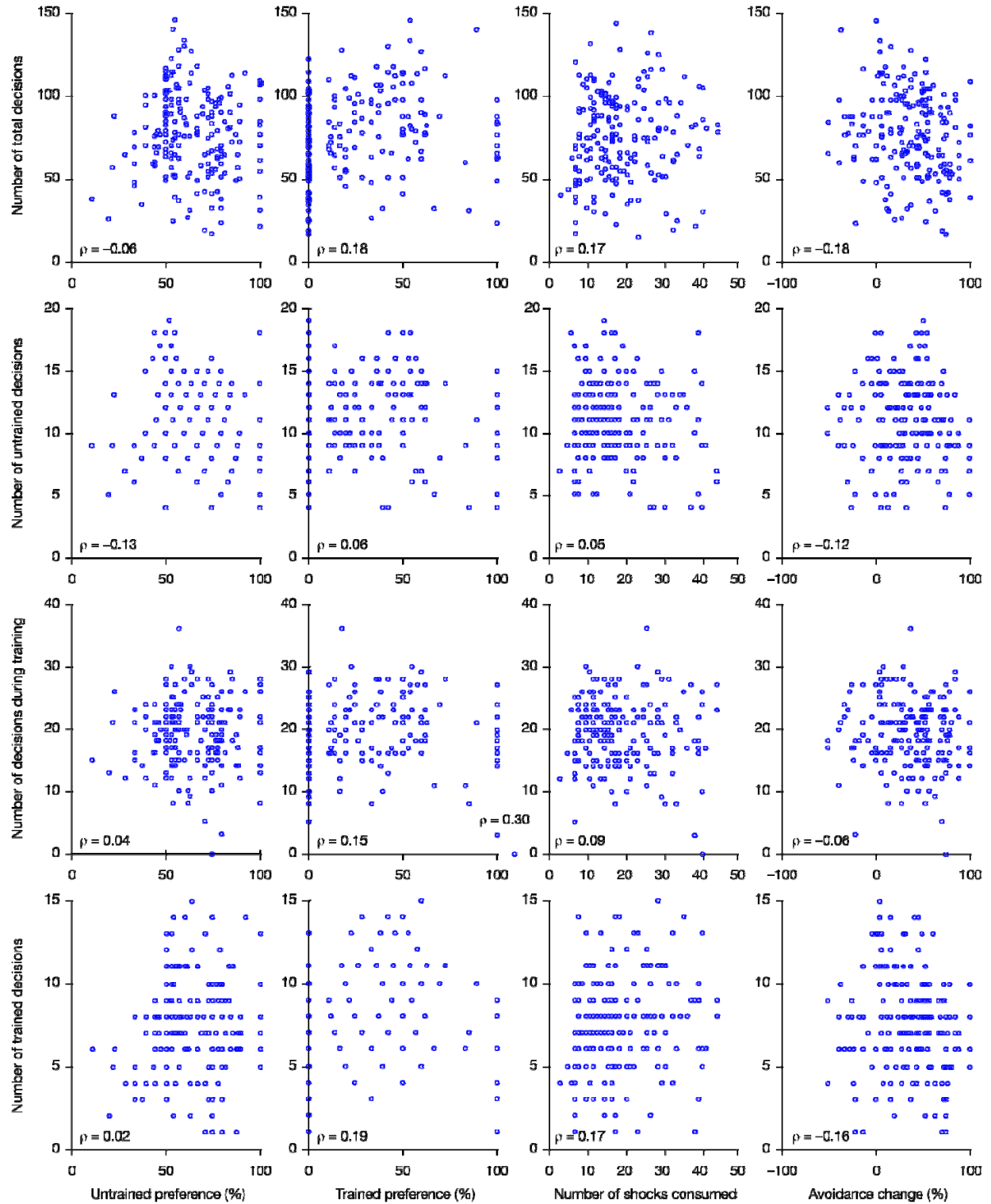


**Figure S4. Relationships of Activity before, during, and after Conditioning with Odor Preference and Learning**

Two hundred flies were trained in an action-contingent regime to avoid MCH; 190 flies met the inclusion criteria for analysis (see Experimental Procedures). Fly

activity was measured as the number of decisions made during the entire 20-min experiment (top row), during 2-min pre- and post-training test periods (second and third row), and during the four 1-min training cycles (bottom row). Activity is largely unrelated to odor preference (left two columns), shock consumption during training (second column from right), and learning (right column). Patterns in the scatterplots arise from the quantized nature of decision scores. Spearman's rank correlation coefficients ( $\rho$ ) reveal only marginal trends among variables, none of which reach statistical significance when the number of tests performed on this data set is taken into account (Bonferroni correction: significance level =  $0.05/16 = 0.003$ ).

**Table S1. Dopaminergic Neurons Labeled by the *TH-GAL4* and *HL9-GAL4* Driver Lines.**

Cell cluster	Anti-TH immunostaining (mean $\pm$ SEM) ( $n = 18$ )	<i>TH-GAL4</i> : <i>UAS-mCD8-GFP</i> (mean $\pm$ SEM) ( $n = 10$ )	<i>HL9-GAL4</i> : <i>UAS-mCD8-GFP</i> (mean $\pm$ SEM) ( $n = 8$ )
PAL	5.2 $\pm$ 0.16	5.1 $\pm$ 0.21	2.89 $\pm$ 0.51
PAM	74.4 $\pm$ 2.10	13.4 $\pm$ 2.80	60.1 $\pm$ 7.54
PPL1	12.1 $\pm$ 0.83	12.1 $\pm$ 1.10	0.89 $\pm$ 0.32
PPL2	6.5 $\pm$ 0.37	5.9 $\pm$ 0.49	3.31 $\pm$ 0.58
PPM1	1.0 $\pm$ 0.00	1.0 $\pm$ 0.00	0.0 $\pm$ 0.00
PPM2	9.7 $\pm$ 0.32	7.3 $\pm$ 0.49	7.86 $\pm$ 0.46
PPM3	8.1 $\pm$ 0.24	7.1 $\pm$ 0.39	1.44 $\pm$ 0.35

Cell numbers in 7 paired dopaminergic clusters were estimated by immunostaining against tyrosine hydroxylase and compared to the fractions of neurons co-expressing mCD8-GFP in the two GAL4 driver lines ( $n$  = brain hemispheres examined).